www.nature.com/npp

American College of Neuropsychopharmacology

ARTICLE

Symptomatic and neurotrophic effects of GABAA receptor positive allosteric modulation in a mouse model of chronic stress

Ashley Bernardo[1], Philip Lee[2], Michael Marcotte[1], Md Yeunus Mian[3], Sepideh Rezvanian[3], Dishary Sharmin[3], Aleksandra Kovačević[4], Miroslav M. Savić[4], James M. Cook[3], Etienne Sibille[1,2,5]✉ and Thomas D. Prevot[1,5]✉

© The Author(s), under exclusive licence to American College of Neuropsychopharmacology 2022

Chronic stress is a risk factor for Major Depressive Disorder (MDD), and in rodents, it recapitulates human behavioral, cellular and molecular changes. In MDD and after chronic stress, neuronal dysfunctions and deficits in GABAergic signaling are observed and responsible for symptom severity. GABA signals predominantly through GABAA receptors (GABAA-R) composed of various subunit types that relate to downstream outcomes. Activity at α2-GABAA-Rs contributes to anxiolytic properties, α5-GABAA-Rs to cognitive functions, and α1-GABAA-Rs to sedation. Therefore, a therapy aiming at increasing α2- and α5-GABAA-Rs activity, but devoid of α1-GABAA-R activity, has potential to address several symptomologies of depression while avoiding side-effects. This study investigated the activity profiles and behavioral efficacy of two enantiomers of each other (GL-II-73 and GL-I-54), separately and as a racemic mixture (GL-RM), and potential disease-modifying effects on neuronal morphology. Results confirm GL-I-54 and GL-II-73 exert positive allosteric modulation at the α2-, α3-, α5-GABAA-Rs and α5-containing GABAA-Rs, respectively, and separately reduces immobility in the forced swim test and improves stress-induced spatial working memory deficits. Using unpredictable chronic mild stress (UCMS), we show that acute and chronic administration of GL-RM provide pro-cognitive effects, with mild efficacy on mood symptoms, although at lower doses avoiding sedation. Morphology studies showed reversal of spine density loss caused by UCMS after chronic GL-RM treatment at apical and basal dendrites of the PFC and CA1. Together, these results support using a racemic mixture with combined α2-, α3-, α5-GABAA-R profile to reverse chronic stress-induced mood symptoms, cognitive deficits, and with anti-stress neurotrophic effects.

Neuropsychopharmacology (2022) 47:1608–1619; https://doi.org/10.1038/s41386-022-01360-y

INTRODUCTION

Chronic stress is a risk factor for psychiatric disorders including Major Depressive Disorder (MDD), displaying mood and cognitive symptoms [1–3]. Interventions to treat depression and other stress-related psychopathologies have focused on the monoaminergic system [4] with limited efficacy on mood symptoms and no efficacy on cognitive symptoms, highlighting unmet clinical needs. Recent studies have focused on the glutamatergic system [5], with promising effects on mood, cognition and cell structure [6, 7]. Similar efficacies were reported with compounds targeting the GABAergic system [8].

Mood and cognitive symptoms result from cellular dysfunctions, altered communication between cells and neuronal atrophy [9–13]. Transcranial magnetic stimulation in MDD patients shows reduced GABAergic function (i.e., cortical inhibition) [14, 15], contributing to impaired excitation/inhibition balance in MDD [16, 17]. Reduced GABA levels are reported in the occipital cortex [18–24], prefrontal cortex (PFC) [25] and anterior cingulate cortex [18, 25–27]. In the PFC, synaptic densities and expression of synaptic function-related genes are reduced [12, 28]. Chronic stress-related disorders [13, 29] and animal models report similar findings [30–32] and demonstrate critical links between prefrontal and hippocampal functions [33]. Chronic stress reduces dendritic length and spine density in the PFC and hippocampus (HPC), likely contributing to cognitive deficits. Of approved treatments, some monoamine-based interventions have reported structural plasticity and remodeling in chronic stress models [34–36], and more recently the NMDA receptor antagonist, ketamine, has shown efficacy at increasing spine density and dendritic complexity in mice, along with antidepressant properties [37]. The neurotrophic effects of ketamine are hypothesized to act through BDNF-TrkB signaling while its fast-acting antidepressant properties are suggested to be initially mediated by activity on GABAergic neurons followed by long-term GABA and glutamate changes [38], highlighting a potential role for GABA in these therapeutic effects.

GABA signals through ionotropic GABAA receptors (GABAA-Rs) and metabotropic GABAB receptors. GABAA-Rs are pentameric ion channels, formed by a combination of 19 subunit subtypes [39]. Drugs acting on GABAA-Rs exist (benzodiazepines or imidazodiazepines), but their use is limited because of side effects (sedation)

[1]Campbell Family Mental Health Research Institute of CAMH, Toronto, Canada. [2]Department of Pharmacology and Toxicology, University of Toronto, Toronto, Canada. [3]Department of Chemistry and Biochemistry, University of Wisconsin–Milwaukee, Milwaukee, USA. [4]Department of Pharmacology, Faculty of Pharmacy, University of Belgrade, Belgrade, Serbia. [5]Department of Psychiatry, University of Toronto, Toronto, Canada. ✉email: Etienne.sibille@camh.ca; thomas.prevot@camh.ca

Received: 23 February 2022 Revised: 17 May 2022 Accepted: 31 May 2022
Published online: 14 June 2022

due to broad activity at several receptor subunits, including α1-GABAA-Rs [40–42]. Studies demonstrated α2-GABAA-Rs, strongly present in the amygdala [43–45] and HPC [43, 46, 47], are linked to regulation of anxious phenotypes [48–52]. The role of α3-GABAA-Rs are not fully characterized, but appear linked to behavioral despair in mice [53]. Other studies link α5-GABAA-Rs with cognitive performances [8, 54, 55], aligned with their preferential expression in cognitive processing regions (HPC and mPFC) [43, 56]. Our group and others showed targeting α5-GABAA-Rs with a positive allosteric modulator (PAM) reverses stress- [55] and age-[57, 58] related cognitive deficits, and chronically reverses age-related neuronal atrophy [8]. Potentiation of α2- and α5-GABAA-Rs, while limiting potentiation of α1-GABAA-R, is hypothesized to improve mood and cognitive symptoms while reducing side effects [40, 59], altogether suggesting potential for treatment of symptomatic and morphological alterations in chronic stress and MDD.

Previously, we showed the α5-PAM GL-II-73, has pro-cognitive and anxiolytic properties, and reduces immobility in the forced swim test (suggesting potential for antidepressant properties in human) at 10 mg/kg IP but not at 5 mg/kg IP [55], and neurotrophic effects at 30 mg/kg PO [58] in mice. However, it remained unknown if its enantiomer, GL-I-54, has similar or complementary properties. Here, we investigated the similarities and/or complementarities of receptor selectivity and behavioral efficacy profile of GL-I-54 and GL-II-73 in stressed mice. We then investigated the symptomatic and neurotrophic potentials of a racemic mixture of both compounds in a mouse model of chronic stress.

MATERIALS AND METHODS

Details provided in the supplementary material.

Compounds

GL-I-54 and GL-II-73 were synthesized as in [60], with >99% chemical and optical purity. GL-RM is a 1:1 mix of each compound.

Electrophysiology

Electrophysiological recordings used HEK-293T cell line transfected with full-length cDNAs for human GABAA-R subtypes α(1/2/3/4/5)β3γ2 [61, 62]. PubMed Protein Sequence repository for GABAA-R subunits reports the binding pocket formed by α1/2/3/5 and γ2 is 100% conserved between mouse and human, predicting similar activity and selectivity across species. Current recordings were performed in absence or presence (5 μM) of GABA. GL-I-54 or GL-II-73 was applied at 0.033–33.33 μM concentrations.

Animals

Seven independent cohorts of 8-week old C57BL/6 mice (50% female) were obtained from Military Medical Academy (Belgrade, Serbia) or Jackson Laboratories (Stock#000664; MA, USA), measuring: pharmacokinetics (#1; $n = 25$), individual enantiomers on elevated plus maze and forced swim test (#2; $n = 24$), effect of GL-I-54 on Y-maze (#3; $n = 42$), GL-I-54 side effects in the rotarod (#4, $n = 18$), and acute (#5; $n = 36$) and chronic (#6; $n = 36$) efficacy of GL-RM and supplementary maximum tolerated dose of GL-I-54 (#7; $n = 18$). Animals were individually housed and maintained on a 12 h light/dark cycle (7:00 ON, 19:00 OFF), with *ad libitum* food and water.

Ethical statement

All animal work was completed in accordance with Ontario Animals for Research Act (RSO 1990, Chapter A.22), Canadian Council on Animal Care (CCAC), Ethical Council for the Protection of Experimental Animals of the Ministry of Agriculture, Forestry and Water Management of the Republic of Serbia, and was approved by the Institutes' Animal Care Committees.

Drug administration

GL-I-54 (1, 3, 5, 10, 30 mg/kg), GL-II-73 (5 mg/kg) or GL-RM (10 mg/kg) were diluted in vehicle solution (85% distilled H_2O, 14% propylene glycol (Sigma Aldrich) and 1% Tween 80 (Sigma Aldrich)) and administered intraperitoneal (IP), 30 min before testing. For oral administration, GL-RM was prepared in tap water (30 mg/kg) and given through drinking water, considering 6 mL average daily fluid intake/animal.

GL-I-54 pharmacokinetics

Mice were treated IP with 3 mg/kg GL-I-54 and euthanized at different time points (5–720 min post-injection) for brain and plasma quantification of ligand by ultraperformance LC-MS/MS (cassette dosing) [63]. In vitro hydrolytic plasma stability of GL-I-54 was tested in vitro at 37 °C, utilizing blank mouse plasma spiked with GL-I-54 and internal standard, as in [64].

Plasma protein and brain tissue binding studies

A rapid equilibrium dialysis assay determined the free fraction of GL-I-54 in mouse plasma and brain tissue as in [65]. GL-I-54-free brain concentrations were calculated by multiplying the total brain concentrations with the appropriate free fractions determined by rapid equilibrium dialysis.

Liver microsomal assay

Metabolic stability was tested in C57BL/6 mouse liver microsomes at 2 μM and 0.5 mg/mL of matrix concentration, as in [66]. NADPH solution, Microsomes/S9 and compounds were added to assay plates. Plates were quenched at T0, 30, 60, and 120 min and assessed in refrigerated LC-MS/MS autosampler. Intrinsic hepatic clearance calculations used 45 mg microsomes/g of liver and 87.5 g liver/kg of body weight for mouse.

Stress paradigms

Two stress paradigms were utilized. The first, chronic restraint stress (CRS), was used with cohorts #2 and #3, consisting of placing mice in a 50 mL Falcon™ Tube for 1 hr twice daily for 1 week. This paradigm consists of a strong stressor that is commonly used for early drug screens. Due to the stress CRS applies, this test is not appropriate for longer (chronic) studies. Therefore, cohorts #5 and #6 were subjected to Unpredictable Chronic Mild Stress (UCMS), a stress paradigm that relies on milder stressors, has slower onset and typically better relates to disease state. These study designs also allow for replication between two different stress paradigms. We used randomized mild stressors (Light modification, cage tilt, predator odor, reduced space, reduce space with odor, restraint, wet bedding, new bedding, no bedding exchange mice or forced bath) twice daily over 6 weeks. Weeks with behavioral testing applied one stressor per day after the behavioral testing (2 weeks). CRS and UCMS animals were housed in a separate room from controls, without environmental enrichment to exacerbate effects of other stressors.

Behavioral tests

Side effects were measured in the rotarod test in cohort #4, assessing locomotor coordination on latency to fall off an accelerating rod over 6 trials and in a maximum tolerated dose-clinical observation study (Supplementary Materials Fig. 4). Mice in cohorts #2 were tested in the elevated plus maze (EPM), measuring avoidance of open arms for 10 min as a proxy of anxiety [67], and in the forced swim test (FST), measuring time spent immobile for 6 min. In cohort #3, mice were exposed to CRS to induce a working memory deficit in the Y maze test, and to test the capacity of reversal of GL-I-54. In cohorts #5 and #6, mice were subjected to UCMS, and each animal's coat state was scored (0 = well-groomed, smooth coat, 1=soiled coat or bald patches) weekly for seven coat regions, as in [68]. Behavioral screen included: anxiety-like avoidance behavior (EPM, open-field, OF; Novelty Suppressed Feeding, NSF; and the Phenotyper Test [67], PT), Sucrose Consumption; (SC), immobility in the FST and cognitive function (Y-maze alternation task [55, 58, 69]).

Tissue collection and golgi staining

Cohort #6 was euthanized by cervical dislocation 24 h after last behavioral test. Brains were immersed in Golgi-Cox staining solution, and assigned a unique identifier (4 brains/group). Brains were shipped to NeuroDigiTech (San Francisco CA, USA) for sectioning (100 μm thickness), mounting and blind quantification of basal and apical dendrites of PFC and CA1 pyramidal cells using NeuroLucida v10 software. Neurons (n = 6/animal) were analyzed for dendritic length, spine number and spine density [70].

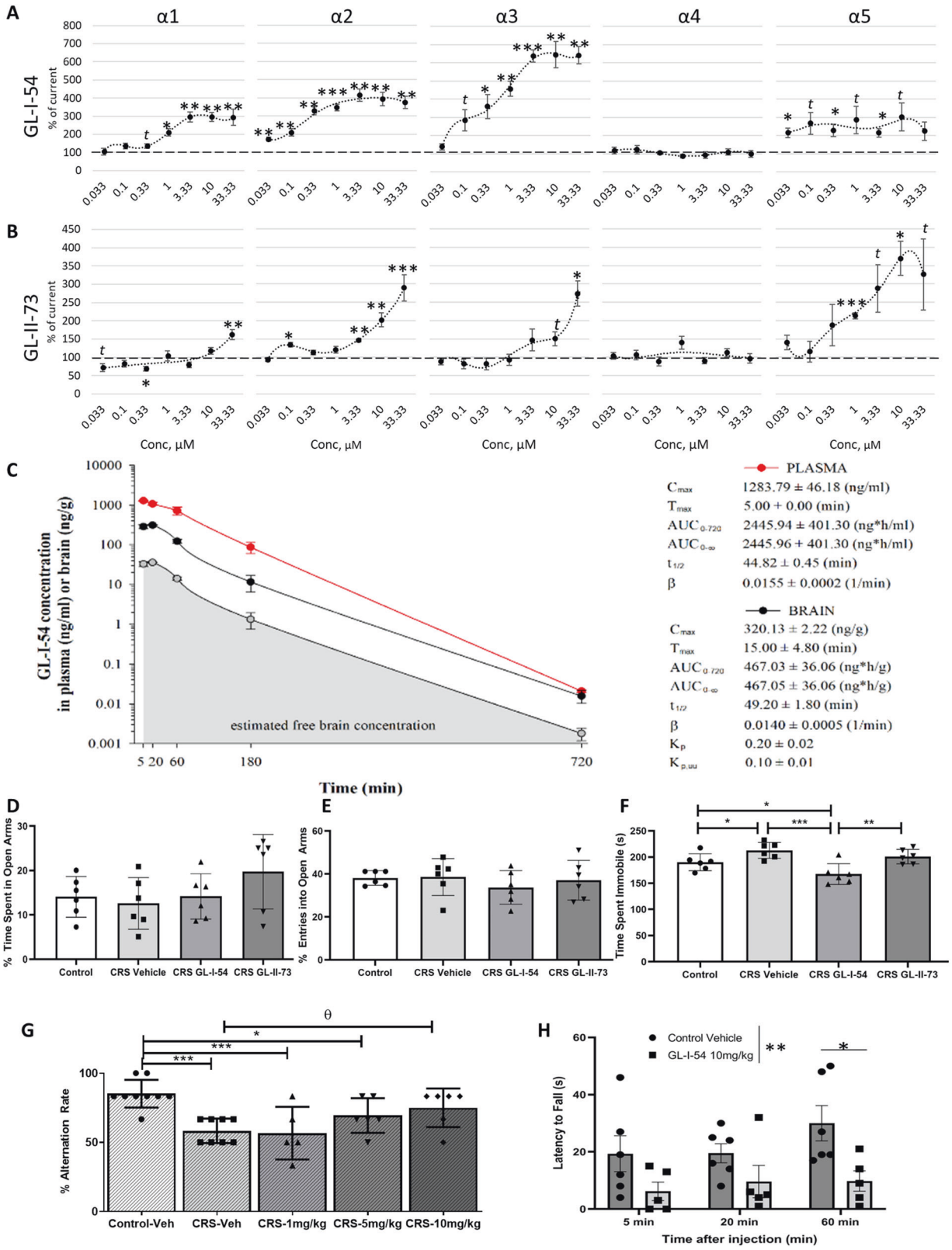

Statistics

Statistical analyses used GraphPad Prism 9. Electrophysiology data and compounds activity at GABAA-R subunits were compared to 100% using t-tests. Other analyzes used two-way ANOVA with concentration and subunit as co-factors, and Bonferroni post-hoc tests. Behavioral analyzes used one-way or two-way ANOVA, and repeated measure ANOVA as relevant. Fishers PLSD tests were used for post-hoc analyses.

Z-scores were calculated to assess consistency of behavioral phenotypes across tests, referred to as z-emotionality using averaged z-scores of behavioral tests as in [71]. Full calculations in supplementary.

Fig. 1 Electrophysiological, pharmacokinetic and behavioral profiles of GL-II-73 and GL-I-54. Electrophysiological recordings were obtained from HEK-293T cells transfected with full-length cDNA for human GABAA receptor subtypes α1β3γ2, α2β3γ2, α3β3γ2, α4β3γ2 or α5β3γ2, in presence of GL-I-54 (**A**) or GL-II-73 (**B**), and in the presence of GABA in the medium (5 μM). Pharmacokinetic profile of GL-I-54 was also examined (**C**). Plasma, brain and free brain concentration-time profile of GL-I-54 after intraperitoneal cassette administration of 3 mg/kg dose in male C57BL/6 mice ($n = 3$ per time point). C_{max}, maximum concentration in plasma or brain; T_{max}, time of maximum concentration in plasma or brain; AUC_{0-720}, area under the plasma or brain concentration-time curve from 0 to 720 min; $AUC_{0-\infty}$, area under the plasma or brain concentration-time curve from 0 to extrapolated infinite time; $t_{1/2}$, elimination half-life from plasma or brain; β, elimination constant rate from plasma or brain; K_p, brain-to-plasma partition coefficient ($K_p = AUC_{0-\infty}$, brain/$AUC_{0-\infty}$, plasma); $K_{p,uu}$, ratio of unbound brain to unbound plasma drug concentrations ($K_{p,uu} = K_p \times$ unbound fraction in brain/unbound fraction in plasma). GL-I-54 and GL-II-73 were then tested in the elevated plus maze and forced swim test at the dose of 5 mg/kg, in mice previously exposed to chronic restraint stress (CRS). Drugs were administered IP, 30 min prior to testing. Percent time spent in the open arms (**D**) and percent entries into open arm (**E**) showed no difference between groups. Time immobile (**F**) showed more time spent immobile in the CRS-Vehicle group, and less time immobile in animals receiving GL-I-54, compared to CRS-Vehicle. GL-II-73 did not show an effect. GL-I-54 was tested in the Y-maze task, assessing working memory (**G**). Animals subjected to CRS and receiving vehicle showed a significant decrease in alternation rate, suggesting a working memory deficit. Animal subjected to CRS and receiving the highest dose of GL-I-54 showed significant increase in alternation rate, suggesting reversal of working memory deficits induced by CRS. Finally, independent mice were tested in the rotarod (**H**; $N = 5$ Control Vehicle and $N = 6$ GL-I-54). Mice were trained to maintain themselves on a rotating rod (rotarod) for 3 trials. Then, they were injected with GL-I-54 at 10 mg/kg, and tested 5 min, 20 min and 60 min past injection time. Latency to fall from the rod was recorded, and showed significant reductions in latency to fall in mice receiving GL-I-54. All values are represented as mean ± standard error of the mean. *$p < 0.05$, **$p < 0.01$, ***$p < 0.001$ compared to 100% in **A**, **B**) or to Control, Control/Vehicle in D-G. $^{\theta}p < 0.05$ compared to CRS-Vehicle.

RESULTS

Statistical significances are provided in Supplementary Tables.

GL-I-54 and GL-II-73 exhibit different GABAA-R potentiation profiles but similar metabolic stability

Both enantiomers were confirmed PAMs, not agonists (Supplementary Fig. 1 and Fig. 1A, B), acting only in the presence of GABA. GL-I-54 significantly increased potentiation at α2-GABAA-Rs (>0.03 μM), α3-GABAA-Rs (>0.33 μM), α1-GABAA-Rs (>1 μM) and α5-GABAA-Rs (0.03, 0.33 and 3.33 μM; Fig. 1A), with preferential activity at α3- and α2- over α1-, α4- and α5-GABAA-Rs (Supplementary Table 1A).

GL-II-73 significantly increased potentiation at α5-GABAA-Rs (>1 μM), α2-GABAA-Rs (3.33 μM), α3-GABAA-Rs (33.33 μM) and α1-GABAA-Rs (33.33 μM; Fig. 1B), with preferential activity at α5-GABAA-Rs over α1-GABAA-Rs (>0.3 μM), α2-GABAA-Rs (between 3.3 and 10 μM), α3-GABAA-Rs (between 1 and 10 μM) and α4-GABAA-Rs (>0.33 μM) (Supplementary Table 1B), confirming data previously published [55].

Pharmacokinetic profile, brain penetrance and stability

Pharmacokinetic profile of GL-I-54 dosed at 3 mg/kg in mice is represented in Fig. 1C (statistical analyses in Supplementary Table 2). Accounting for the doses administered in respective studies, GL-I-54 and GL-II-73 exhibit comparable pharmacokinetic patterns. As a representative example, 20 min after the 3 mg/kg dose, GL-I-54 achieved 311.75 ± 6.72 ng/g, while GL-II-73 reached 264.61 ± 38.22 ng/g (Supplementary Fig. 2). After appropriate adjustments (for the 5 mg/kg dose, free fraction, brain tissue density and unit), these close-to-maximum concentrations achievable in the mouse brain correspond to the 0.100–0.330 μM concentration range in electrophysiological recordings (calculation in Supplementary Fig. 2). This implies that, in acute behavioral experiments with 5 mg/kg dose, GL-I-54 likely potentiates α_1, α_2, α_3 and α_5 GABAA-Rs, however, α_1 potentiation is mild. 5 mg/kg of GL-II-73, on the other hand, is fairly silent on all GABAA-Rs, with the potential to mildly activate α_2 and α_5 receptors; on α_1 and α_3 receptors, nevertheless, it behaves as a null modulator. Plasma and brain free fractions of GL-I-54 were 22.57% and 11.49%, respectively, while, as previously reported for GL-II-73 were 20.39% and 12.14% [55], respectively. Brain to plasma ratio (K_p) evaluates brain penetrance (penetrant when $K_p > 0.04$). GL-I-54 is brain penetrant ($K_p = 0.20$), similarly to GL-II-73 ($K_p = 0.30$), which is further supported by the ratio of unbound brain to unbound plasma ligand concentrations values, $K_{p,uu}$ (0.10 vs 0.18, respectively). GL-I-54 displayed high in vitro metabolic stability, although lower compared to GL-II-73; after 4 h of incubation in mouse plasma, the fraction of remaining intact ligand was 78.41% (vs 98.88% of GL-II-73 [55]). In the liver microsomal assay, GL-I-54 showed a 198 min half-life with 70% remaining after 2 h. Intrinsic hepatic clearance was 27.6 mL/min/kg. GL-II-73 showed a longer half-life, 256 min, with 75.6% remaining after 2 h. Intrinsic hepatic clearance was 21.3 mL/min/kg.

Acute administration of GL-I-54 displays anxiolytic effects and reverses spatial working memory deficits in the chronic restrain stress model with locomotor side effects at higher dose

In mice subjected to CRS, GL-I-54 (5 mg/kg) and GL-II-73 (5 mg/kg) were tested for their effects on anxiety-related avoidance in the elevated plus maze (EPM), and on immobility in the forced swim test (FST). Effects on spatial working memory were tested in the Y-maze (5 mg/kg and 10 mg/kg). After CRS, GL-I-54 and GL-II-73 had no effect on percent time in open arms of the EPM or percent entries into open arms (Fig. 1D, E; and Supplementary Table 2). In the FST, CRS increased time spent immobile, which was significantly reversed by GL-I-54 (Fig. 1F), suggesting GL-I-54 reverses stress-induced increase in immobility in this test. Interestingly, GL-I-54 given in non-stressed animals at the dose of 5 mg/kg showed a trend at increasing time in the open arm in the EPM, and significantly reduced time spent immobile in the FST (Supplementary Fig. 3). In the Y-maze, CRS induced an alternation rate deficit that was reversed by GL-I-54 at 10 mg/kg but not 5 mg/kg (Fig. 1G), suggesting the capacity of reversing spatial working memory deficits. Locomotor side effects of GL-I-54 at 10 mg/kg were tested in the rotarod (Fig. 1H, and Supplementary Table 2) to support previous finding from a maximum tolerated dose-clinical observation study demonstrating sedative properties of GL-I-54 (Supplementary Fig. 4). Decreasing latency to fall 60 min after injection was found, suggesting sedation at this dose.

Acute administration of GL-RM reverses spatial working memory deficits in the UCMS model

Based on the selective effects observed with acute administration of GL-I-54 or GL-II-73 alone at 5 mg/kg, we tested potential additive effects and low side effects using a 1:1 racemic mixture of 5 mg/kg each, called GL-RM, in the UCMS model (Fig. 2A; and Supplementary Table 3), with a final GL-RM dose of 10 mg/kg. Weekly monitoring showed UCMS deteriorated coat state, not reversed by acute treatment, weight gain remained unaffected (Supplementary Fig. 5). Using the Phenotyper, no locomotor activity differences were detected between groups with GL-RM injection supporting its lack of sedative effects (Supplementary Fig. 6).

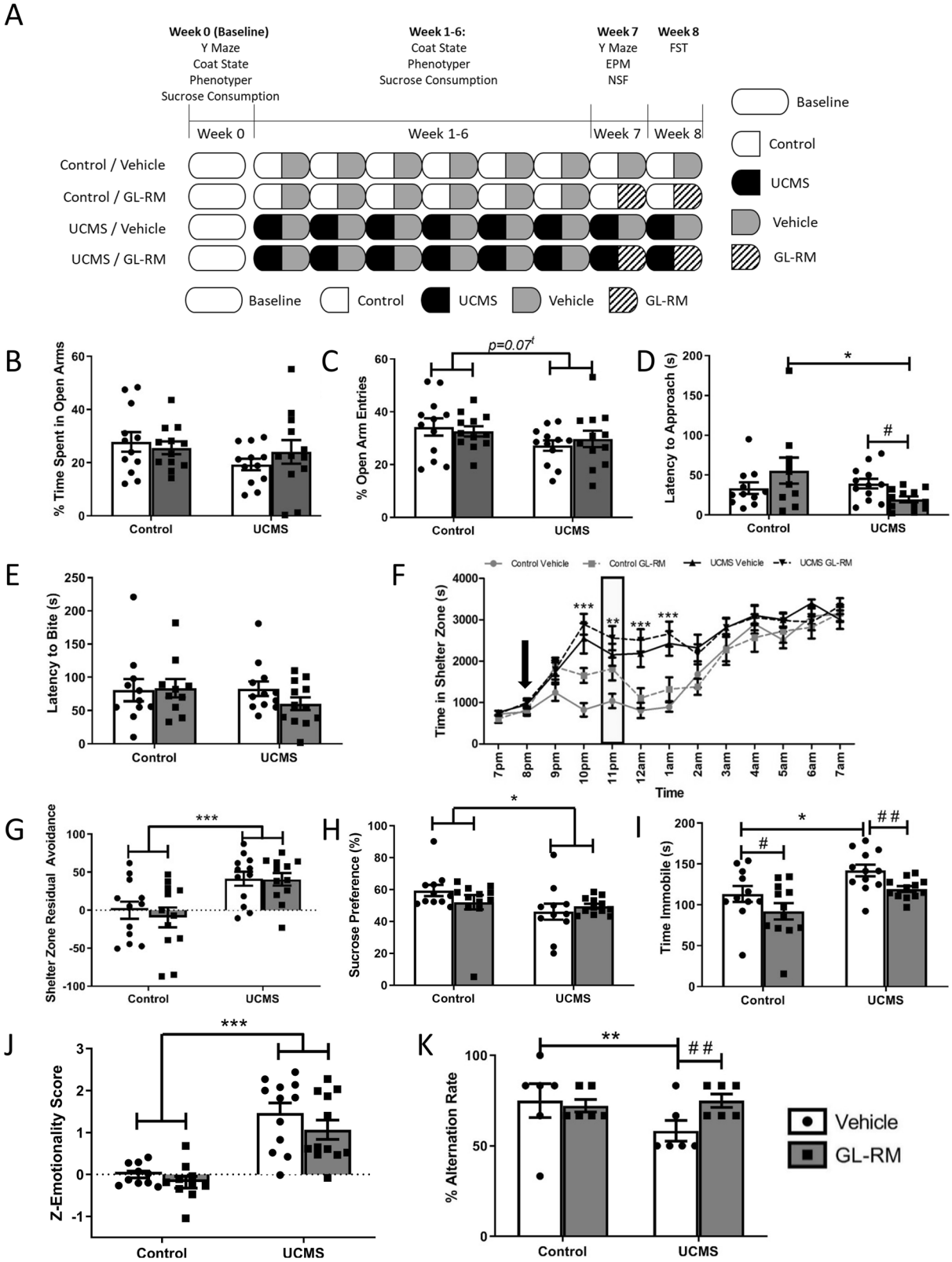

In the EPM, there was no effect of UCMS or treatment on percent time in open arms (Fig. 2B). There was a trend level effect of stress reducing the percent of entries into open arms but no effect of treatment (Fig. 2C). NSF latency to approach found a significant interaction between UCMS and treatment, due to reduced latency in UCMS + GL-RM treated animals compared to Control+GL-RM and compared to UCMS + vehicle (Fig. 2D), suggesting anxiolytic properties through reduced avoidance. Latency to bite was unaffected by UCMS or treatment (Fig. 2E). Phenotyper test and associated measure of residual avoidance

Fig. 2 Effect of acute treatment of GL-RM on anxiety, emotionality and working memory deficits in mice subjected to chronic stress. Male and female mice were tested at baseline in the Y-maze, the phenotyper and the sucrose consumption test prior to being subjected to 6 weeks of UCMS (**A**). Weekly, mice were tested in the phenotyper test, the sucrose consumption and their weight and coat state were measured. After 6 weeks of UCMS, acute injections were performed 30 min prior to behavioral testing. In the elevated plus maze, time spent (**B**) and entries (**C**) in the open arms were measured, with no significant effect of UCMS, treatment or interaction. In the novelty suppressed feeding test, latency to approach (**D**) and latency to bite (**E**) were assessed. Statistical analyses showed that acute GL-RM treatment reduces latency to approach in mice subjected to UCMS. In the phenotyper test (**F**), mice were placed in the box overnight, where a stressful stimulus was applied at 11 pm, for 1 h. Time spent in the shelter zone showed that mice subjected to UCMS spent more time in the shelter than control mice. Calculating a residual avoidance score (**G**), statistical analyses showed a significant increase in residual avoidance in mice subjected to UCMS. In the sucrose consumption test (**H**), mice subjected to UCMS showed a significant decrease in preference to sucrose. In the forced swim test (**I**), mice subjected to UCMS showed increased immobility, while mice treated with GL-RM showed a reduction in immobility. Combining the individual score into a global z-score (**J**), statistical analyses confirmed a significant impact of UCMS, with reduced effect of GL-RM. Finally, mice were tested in the Y-maze (**K**), where statistical analyses showed altered alternation with UCMS, which is reversed by acute GL-RM treatment. $^{*}p < 0.05$, $^{**}p < 0.01$, $^{***}p < 0.001$ effect of UCMS, $^{\#}p < 0.05$, $^{\#\#}p < 0.01$ effect of GL-RM.

used in Prevot et al. [67] assess anxiety-related avoidance weekly. The residual avoidance score captures the time spent in the shelter, after a 1 h-light challenge, measuring residual avoidance of the previously-lit zone. Prior to UCMS, there was no group difference (Supplementary Fig. 7A, B). Upon UCMS, residual time spent in the shelter following an acute light challenge was increased (Fig. 2F, G; Supplementary Fig. 7C–G). On week 6, acute GL-RM treatment did not affect time in the shelter after the light challenge (Fig. 2F). Sex-dependent analyses showed males spent more time in the shelter than females (data not shown).

At week 6, sucrose preference was significantly reduced by UCMS but unaffected by GL-RM (Fig. 2H, and Supplementary Table 3), suggesting a lack of effect from treatment at reversing UCMS-induced reduced sucrose preference. In the FST, UCMS increased time immobile, which was reduced by GL-RM (Fig. 2I). Z-scoring of behavioral emotionality, integrating behavioral outcomes in a single readout confirmed the effect of UCMS, and a limited efficacy of acute GL-RM treatment (Fig. 2J). In contrast, the Y-maze spatial working memory deficit induced by UCMS was significantly reversed by acute GL-RM treatment (Fig. 2K).

Altogether, these results showed that acute administration of GL-RM mainly overcomes spatial working memory deficits induced by UCMS, while having reduced efficacy on emotionality.

Chronic GL-RM conserves spatial working memory benefits in the UCMS model

The effects of chronic GL-RM administration were investigated in mice subjected to UCMS (Fig. 3A). Altered coat state and reduced weight gain with UCMS was significant from week 1–6, with no effect on chronic GL-RM (Supplementary Fig. 8).

There was no effect of UCMS or treatment in the EPM, OF and NSF latency to approach (Fig. 3B–F, and Supplementary Table 4). Latency to bite found an effect of UCMS and treatment. Unexpectedly, UCMS + GL-RM mice compared to Control + GL-RM mice showed decreased latency to bite (Fig. 3G). In the Phenotyper test (Fig. 3H and Supplementary Fig. 9), UCMS increased residual avoidance in the shelter zone, while chronic GL-RM was trending to decrease it.

Sucrose preference was unaffected by UCMS, but chronic GL-RM increased preference (Fig. 3I). In the FST, the time spent immobile was unaffected by UCMS or treatment (Fig. 3J). UCMS significantly increased z-emotionality, with a trend level effect of chronic GL-RM reducing z-emotionality (Fig. 3K).

In the Y-maze, UCMS decreased percent alternation rate (Control + Vehicle vs UCMS + Vehicle) and chronic GL-RM significantly increased percent alternation rate between UCMS + vehicle and UCMS + GL-RM groups (Fig. 3L), confirming efficacy at reversing stress-induced spatial working memory deficits.

Results suggest that chronic GL-RM may contribute to reducing z-emotionality, with discrete effects on individual outcomes, and confirm its effect at reversing UCMS-induced spatial working memory deficits.

Chronic GL-RM administration reverses neuronal morphology deficits induced by UCMS

We quantified morphological changes in apical and basal dendrites of PFC pyramidal neurons (Fig. 4A–C, and Supplementary Fig. 10). Dendritic length was not affected by UCMS or treatment, but spine count and spine density were significantly lower in UCMS compared to control mice (Fig. 4D, E, and Supplementary Fig. 10). Such decreases were reversed by chronic GL-RM in basal and apical segments, with spine density in apical PFC dendrites of GL-RM treated UCMS animals being significantly higher than UCMS animals and not significantly different from controls (Fig. 4D).

Similarly, significant UCMS effects on spine density and reversal by chronic GL-RM treatment were observed in CA1 pyramidal neurons (Fig. 4E, and Supplementary Fig. 11).

Improved cognitive functions might be related to improved spine density and overall neuronal morphology (Supplementary Table 5 and Supplementary Fig. 12), although studies with larger sample size are required to confirm this hypothesis.

DISCUSSION

This work is based on observations that patients with psychopathologies related to chronic stress exposure experience mood and cognitive deficits, while current treatments display moderate-to-no efficacy for mood and cognition [1–3, 9]. We investigated the efficacy of two enantiomers with activity at α3-, α2-, α5-GABAA-Rs (GL-I-54) and α5-GABAA-Rs (GL-II-73) separately, and in combination (GL-RM) at alleviating such symptoms and neuronal atrophy in CRS and UCMS models. GL-I-54 reduced immobility in the FST, did not show efficacy in the EPM, nor reversed stress-induced working memory deficits at low dose (5 mg/kg). GL-I-54 required a higher dose (10 mg/kg) to reverse working memory deficits though while causing slight sedation. GL-II-73 previously showed no effect on working memory at doses lower than 10 mg/kg [55]. Acute and chronic treatment of a racemix combination of both enantiomers (GL-RM) improved stress-induced working memory deficits. Acute GL-RM only decreased immobility in the FST, suggesting inconclusive results on emotionality. Finally, chronic GL-RM treatment reversed the UCMS-induced reduction in spine densities in the PFC and CA1 of UCMS mice, with morphological measures correlating with improvement of emotionality and working memory.

Racemic mixtures have therapeutic relevance by harnessing different enantiomer GABAA-R specificities

Therapeutic development often favors pure substances over racemic mixtures due to superior selectivity and reduced off-target activities [72, 73]. Racemic development becomes justified if therapeutic benefits of each enantiomer are similar, complimentary or devoid of side-effects and toxicity [74]. GL-RM harnessed the similar, yet unique selectivity profiles of GL-I-54 and GL-II-73 to

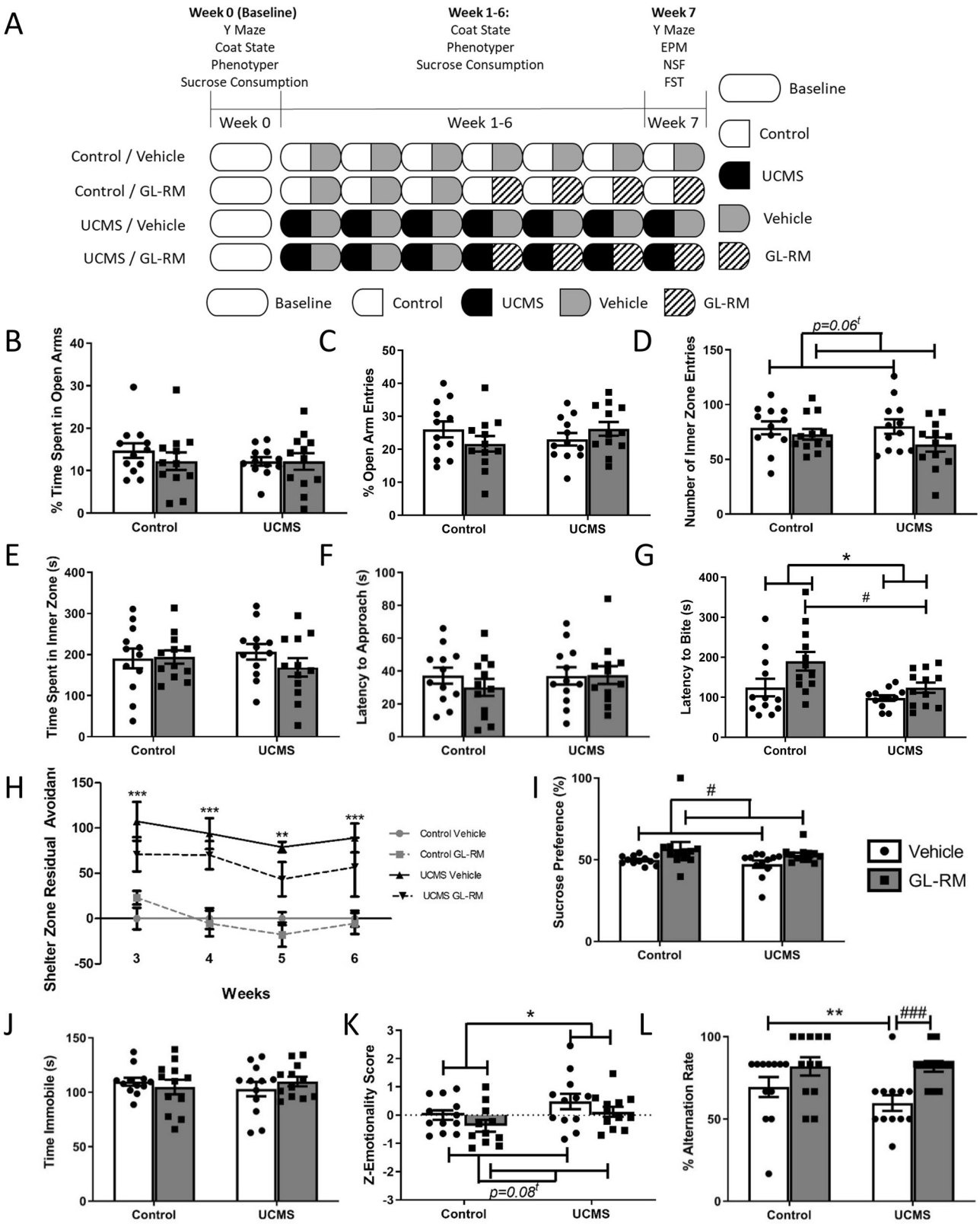

target the GABAA-Rs known to be involved in anxiety, depression and cognition. GL-I-54 displays activity at α3-, α2-, α5-, α1-GABAA-Rs while GL-II-73 confirmed preferential activity at α5-GABAA-Rs [55], likely reflecting different interactions of each compound's conformation in the binding pocket.

Racemic mixtures are not uncommon in the treatment of MDD [75, 76]. Fluoxetine [75, 77], citalopram [78] or ketamine [37] are clinically used racemic antidepressants [75, 79, 80]. Racemic R,S-ketamine has more efficacy than non-racemic S-Ketamine [81]. Racemic therapies can harness broader selectivity profiles to

Fig. 3 Effect of chronic treatment of GL-RM on anxiety, emotionality and working memory deficits in mice subjected to chronic stress. Male and female mice were tested at baseline in the Y-maze, the phenotyper and the sucrose consumption test prior to being subjected to 6 weeks of UCMS (**A**). After 3 weeks of UCMS, chronic treatment with GL-RM in the drinking water was initiated, for a total of 4 weeks. Weekly, mice were tested in the phenotyper test, the sucrose consumption and their weight and coat state were measured. After 6 weeks of UCMS, and 3 weeks of treatment, mice were tested in the elevated plus maze. Time spent (**B**) and entries (**C**) in the open arms were measured, but did not show statistical differences. Mice were also tested in the open field for the time spent (**D**) and number of entries (**E**) in the inner zone. Again, statistical analyses did not reveal any effect of UCMS nor treatment. In the novelty suppressed feeding test, latency to approach (**F**) and latency to bite (**G**) were assessed. Mice were tested in the Phenotyper weekly, and the residual avoidance scores from week 3 to 6 were analyzed, since the treatment was onboard during these testing periods (**H**). In the sucrose consumption test (**I**), mice receiving chronic GL-RM showed a significant increase in preference to sucrose. In the forced swim test (**J**), statistical analyses did not reveal significant differences between groups. Combining the individual score into a global z-score (**K**), statistical analyses confirmed a significant impact of UCMS at increasing emotionality, with a trend level effect ofchronic GL-RM reducing emotionality. Finally, mice were tested in the Y-maze (**L**), where statistical analyses showed altered alternation with UCMS, which is reversed by acute GL-RM treatment. $^{*}p < 0.05$, $^{**}p < 0.01$, $^{***}p < 0.001$ effect of UCMS, $^{\#}p < 0.05$, $^{\#\#\#}p < 0.001$ effect of GL-RM.

address multiple pathophysiological mechanisms but have the added risk of off-target side effects. In vivo, considering estimated free concentrations in the brain after a 5 mg/kg dose, we found that concentration is slightly above 100 nM. At this concentration, GL-I-54 may act as a PAM at non-α1 GABAARs, while GL-II-73 would mainly have only slight PAM activity at α2- and α5-GABAA-Rs, and be a null modulator at α1-GABAA-Rs. When combined together, low concentrations of GL-II-73 may be effective as an "on-site softener" of activity of GL-I-54, especially at α1-GABAA-Rs, limiting binding of GL-I-54 in the binding pocket and therefore limiting negative effects observed when potentiating this subunit, further suggesting GL-RM as an intervention for a more complete treatment of depression symptomatology.

Targeting α2-, α3-, α5-GABRA-Rs with GL-RM displays superior efficacy on spatial working memory at lower concentrations than individual enantiomers

Reconciling potentiation profiles with behavioral results, we compared GL-I-54 and GL-II-73 alone at 5 mg/kg or 10 mg/kg after CRS to GL-RM 10 mg/kg (each enantiomer at 5 mg/kg) after UCMS. At 5 mg/kg, GL-I-54 reduced immobility in the FST. Previously reported, GL-II-73 only reduced immobility at 10 not 5 mg/kg [55]. Acute GL-RM reduced UCMS-exposed animal immobility in the FST suggesting GL-RM retains this effect likely due to GL-I-54 activity. GL-RM also reduced immobility in non-stressed animals showing effects at baseline and in the absence of UCMS. Neither enantiomer showed significant efficacy on avoidance behavior, separately or in combination (GL-RM).

Interestingly, GL-RM combined the efficacy of both enantiomers for pro-cognitive effects, specifically spatial working memory. While neither enantiomer elicited pro-working memory effects at 5 mg/kg alone, their combined activity in GL-RM improved working memory deficits. This could be the result of an additive effect of the two compounds at GABAA-Rs, or a reduction of a putative amnestic effect caused by α1-GABAA-R null potentiation [82] with the use of a low GL-II-73 dose. Nevertheless, this finding demonstrates a clinical advantage for using GL-RM over either pure enantiomer at low concentrations, avoiding side effects and benefiting from combined profiles.

Chronic GL-RM administration has neurotrophic effects

As in MDD, chronic stress leads to reduced synchronicity between the PFC and HPC, and dysfunctional information processing within cortical and hippocampal structures [83]. Dendritic length and spine density are reduced in the PFC and HPC of MDD patients and stressed mice [84], contributing to cognitive deficits. Our findings are consistent with other UCMS studies reporting neuronal atrophy and working memory deficits [85–87]. We previously showed that chronic administration of GL-II-73 alone remedies age-related spine loss in pyramidal neurons, through α5-GABAA-R modulation was confined to apical dendrites [58], where α5-GABAA-Rs are primarily located [88–90], and consistent with GL-II-73 preferentially potentiating α5-GABAA-Rs. With GL-RM, neurotrophic effects were extended to basal segments in both PFC and HPC, suggesting a potential role of α2- and/or α3-GABAA-Rs in this neurotrophic effect. Previously, α5- and α2-GABAA-Rs have been implicated in dendritic outgrowth, spine maturation and synapse formation [91–93], thus their modulation by GL-RM may be responsible for spine density restoration at apical and basal dendrites.

While showing spine count improvements, it remains unclear whether spines are prevented from shrinking, or if they are generated *de novo*. Ketamine showed ability to overcome stress hormone-induced spine loss by a combination of restored spines and *de novo* spines, with some preference for *de novo* [94]. A similar combination may also be the case for GL-RM. Evidence that GL-RM has an effect at a pathophysiological level (not only symptomatic levels) is substantially valuable for translational efficacy within humans.

Limitations

In our primary drug screening, the lack of a non-stress group receiving GL-I-54 does not allow us to know baseline effects of GL-I-54 in the Y maze. However, non-stressed animals perform at 80% accuracy, which leaves very little room for improvement, so other tests should be considered for baseline testing. In the GL-RM studies, we see that GL-RM administered in non-stressed animals does not have an effect, and previous studies from our group showed that GL-II-73 alone does not have an effect in the Y maze [55]. Therefore, we can anticipate that GL-I-54 does not have an effect alone, in non-stressed mice, but testing or validation in other tests would confirm this. In addition, we tested GL-RM on a single cognitive domain, but cognitive deficits in depression extend beyond spatial working memory and exploring others is needed for future experiments. Regarding neurotrophic effects, we investigated the PFC and HPC for their regulation of stress-related and depressive symptoms. It could be valuable to investigate how GL-RM modulates connectivity in subnuclei of the amygdala, potentially decreasing the hyperactivity/increased connectivity reported after chronic stress [95, 96]. We used chronic stress models because they recapitulate behavioral and cellular changes observed in human depression [97–100]. While using the most commonly reported stressors [101], variability in anxiety-related outcomes limited clear conclusions on procedure and treatment, not uncommon in behavioral studies [67, 102]. The Phenotyper test measuring context anxiety [67] provided insight to anxiolytic properties of GL-RM with better consistency. The discrepancy between EPM/NSF and Phenotyper results highlight potential biases from hands-on behavioral assays versus automatized approaches [103].

To conclude, the therapeutic relevance of a targeted PAM approach at GABAA-Rs is reinforced and the role of α5-GABAA-Rs in cognition is supported. At low-to-moderate dose, both compounds, used together, show promising effects for the treatment of mood and cognitive symptoms, as well as morphological changes in disorders such as MDD.

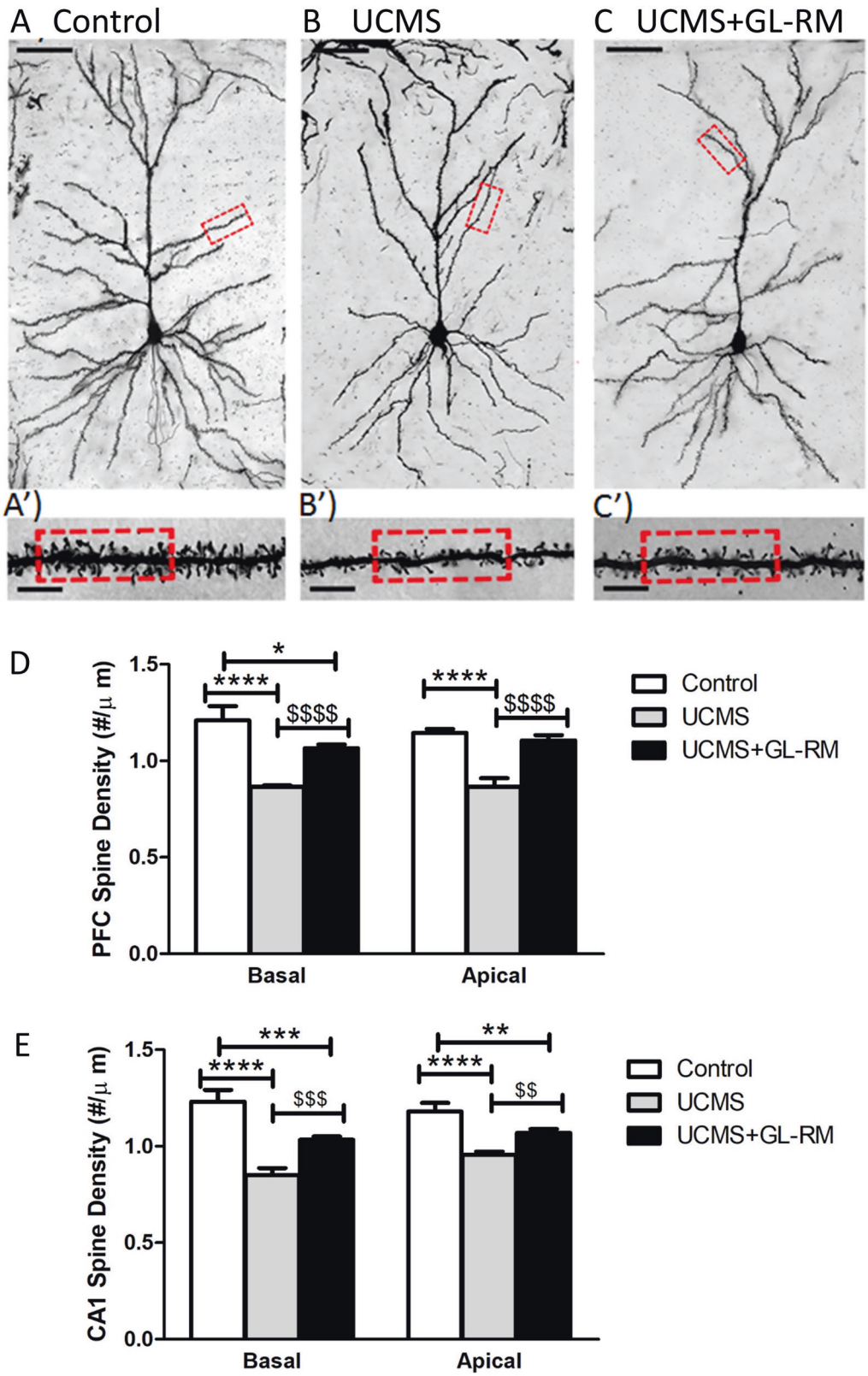

Fig. 4 Chronic treatment with GL-RM reverses chronic-stress induced spine density reduction in the PFC and the CA1. After completion of the behavioral screening, mice were euthanized and brains were stained with Golgi-Cox solution. Pyramidal neurons ($N = 6$ per mouse) from 4 mice per group (**A**–**C**) were analyzed for dendritic length, spine counts and spine density. Basal and apical spine densities were measured in the PFC (**D**) and the CA1 of the hippocampus (**E**). ANOVA in the basal and apical segments revealed significant differences between groups, in both brain regions. This difference was explained by a decrease in spine density in mice subjected to UCMS compared to Control mice that was partially reversed by chronic treatment with GL-RM. $^{*}p < 0.05$, $^{**}p < 0.01$, $^{***}p < 0.001$, $^{****}p < 0.0001$ compared to "Control"; $^{\$\$}p < 0.01$, $^{\$\$\$}p < 0.001$, $^{\$\$\$\$}p < 0.0001$ compared to "UCMS". Scale bar in (**A**–**C**) represents 50 μm.

REFERENCES

1. MacQueen GM, Memedovich KA. Cognitive dysfunction in major depression and bipolar disorder: Assessment and treatment options. Psychiatry Clin Neurosci. 2017;71:18–27.
2. Malhi GS, Mann JJ. Depression. Lancet. 2018;392:2299–312.
3. Gartlehner G, et al. Pharmacological and non-pharmacological treatments for major depressive disorder: review of systematic reviews. BMJ Open. 2017;7: e014912.
4. Hirschfeld RMA. History and evolution of the monoamine hypothesis of depression. J Clin Psychiatry. 2000;61(Suppl 6):4–6.
5. Xia C-Y, et al. Targeting the dysfunction of glutamate receptors for the development of novel antidepressants. Pharmacol Therapeutics. 2021;226:107875.
6. Davis MT, et al. Acute cognitive effects of single-dose intravenous ketamine in major depressive and posttraumatic stress disorder. Transl Psychiatry. 2021;11:205.
7. Gill H, et al. The effects of ketamine on cognition in treatment-resistant depression: A systematic review and priority avenues for future research. Neurosci Biobehav Rev. 2021;120:78–85.
8. Prevot T, Sibille E. Altered GABA-mediated information processing and cognitive dysfunctions in depression and other brain disorders. Mol Psychiatry. 2021;26:151–67.
9. Duman CH, Duman RS. Spine synapse remodeling in the pathophysiology and treatment of depression. Neurosci Lett. 2015;601:20–9.
10. Williams LM. Precision psychiatry: A neural circuit taxonomy for depression and anxiety. Lancet Psychiatry. 2016;3:472–80.
11. Banasr M, Dwyer JM, Duman RS. Cell atrophy and loss in depression: Reversal by antidepressant treatment. Curr Opin Cell Biol. 2011;23:730–7.
12. Kang HJ, et al. Decreased expression of synapse-related genes and loss of synapses in major depressive disorder. Nat Med. 2012;18:1413–7.
13. Holmes SE, et al. Lower synaptic density is associated with depression severity and network alterations. Nat Commun. 2019;10:1529.
14. Lissemore JI, et al. Reduced GABAergic cortical inhibition in aging and depression. Neuropsychopharmacology. 2018;43:2277–84.
15. Lee JC, et al. The role of transcranial magnetic stimulation in treatment-resistant depression: A review. Curr Pharm Des. 2012;18:5846–52.
16. Fogaca MV, Duman RS. Cortical GABAergic dysfunction in stress and depression: New insights for therapeutic interventions. Front Cell Neurosci. 2019;13:87.
17. Newton, DF, et al. Chapter 28 - Altered GABAergic Function, Cortical Microcircuitry, and Information Processing in Depression, in Neurobiology of Depression, J Quevedo, AF Carvalho, and CA Zarate, Editors. 2019, Academic Press. p. 315–29.
18. Bhagwagar Z, et al. Low GABA concentrations in occipital cortex and anterior cingulate cortex in medication-free, recovered depressed patients. Int J Neuropsychopharmacol/Off Sci J Collegium Int Neuropsychopharmacologicum (CINP). 2008;11:255–60.
19. Goddard AW, et al. Reductions in occipital Cortex GABA levels in panic disorder detected with 1H-Magnetic resonance spectroscopy. Arch Gen Psychiatry. 2001;58:556–556.
20. Price RB, et al. Amino acid neurotransmitters assessed by proton magnetic resonance spectroscopy: Relationship to treatment resistance in major depressive disorder. Biol Psychiatry. 2009;65:792–800.
21. Sanacora G, et al. Subtype-specific alterations of gamma-aminobutyric acid and glutamate in patients with major depression. Arch Gen Psychiatry. 2004;61:705–13.
22. Sanacora G, et al. Increased occipital cortex GABA concentrations in depressed patients after therapy with selective serotonin reuptake inhibitors. Am J Psychiatry. 2002;159:663–5.
23. Sanacora G, et al. Subtype-specific alterations of gamma-aminobutyric acid and glutamate in patients with major depression. Arch Gen Psychiatry. 2004;61:705–13.
24. Sanacora G, et al. Reduced cortical γ-Aminobutyric acid levels in depressed patients determined by proton magnetic resonance spectroscopy. Arch Gen Psychiatry. 1999;56:1043–1043.
25. Hasler G, et al. Reduced prefrontal glutamate/glutamine and gamma-aminobutyric acid levels in major depression determined using proton magnetic resonance spectroscopy. Arch Gen Psychiatry. 2007;64:193–200.
26. Gabbay V, et al. Anterior cingulate Cortexγ-Aminobutyric acid in depressed adolescents. Arch Gen Psychiatry. 2012;69:139–139.
27. Plante DT, et al. Reduced gamma-aminobutyric acid in occipital and anterior cingulate cortices in primary insomnia: A link to major depressive disorder? Neuropsychopharmacology. 2012;37:1548–57.
28. Feyissa AM, et al. Reduced levels of NR2A and NR2B subunits of NMDA receptor and PSD-95 in the prefrontal cortex in major depression. Prog Neuro-Psychopharmacol Biol Psychiatry. 2009;33:70–75.
29. Christoffel DJ, Golden SA, Russo SJ. Structural and synaptic plasticity in stress-related disorders. Rev Neurosci. 2011;22:535–49.
30. Izquierdo A, Wellman CL, Holmes A. Brief uncontrollable stress causes dendritic retraction in infralimbic cortex and resistance to fear extinction in mice. J Neurosci. 2006;26:5733–8.
31. Liston C, et al. Stress-induced alterations in prefrontal cortical dendritic morphology predict selective impairments in perceptual attentional set-shifting. J Neurosci. 2006;26:7870–4.
32. Shansky RM, et al. Stress-induced dendritic remodeling in the prefrontal cortex is circuit specific. Cereb Cortex. 2009;19:2479–84.
33. Abdallah CG, et al. Prefrontal cortical GABA abnormalities are associated with reduced hippocampal volume in major depressive disorder. Eur Neuropsychopharmacol. 2015;25:1082–90.
34. Bessa JM, et al. The mood-improving actions of antidepressants do not depend on neurogenesis but are associated with neuronal remodeling. Mol Psychiatry. 2009;14:764–73.
35. Ampuero E, et al. Chronic fluoxetine treatment induces structural plasticity and selective changes in glutamate receptor subunits in the rat cerebral cortex. Neuroscience. 2010;169:98–108.
36. Lyttle K, et al. Repeated fluvoxamine treatment recovers juvenile stress-induced morphological changes and depressive-like behavior in rats. Brain Res. 2015;1616:88–100.
37. Phoumthipphavong, V, et al., Longitudinal effects of ketamine on dendritic architecture in vivo in the mouse medial frontal cortex. eNeuro, 2016. 3: p. *ENEURO*.0133-15.2016.
38. Gerhard DM, et al. GABA interneurons are the cellular trigger for ketamine's rapid antidepressant actions. J Clin Invest. 2020;130:1336–49.
39. Mohler H. GABA(A) receptor diversity and pharmacology. Cell Tissue Res. 2006;326:505–16.
40. Sigel E, Ernst M. The Benzodiazepine binding sites of GABAA receptors. Trends Pharmacol Sci. 2018;39:659–71.
41. Pariente A, et al. The Benzodiazepine–dementia disorders link: Current state of knowledge. CNS Drugs. 2016;30:1–7.
42. Sieghart W, Savić MM. International Union of basic and clinical pharmacology. CVI: GABA(A) Receptor subtype- and function-selective ligands: Key issues in translation to humans. Pharm Rev. 2018;70:836–78.
43. Fritschy JM, Mohler H. GABAA-receptor heterogeneity in the adult rat brain: differential regional and cellular distribution of seven major subunits. J Comp Neurol. 1995;359:154–94.
44. Geracitano R, et al. Functional expression of the GABA(A) receptor α2 and α3 subunits at synapses between intercalated medial paracapsular neurons of mouse amygdala. Front Neural Circuits. 2012;6:32.
45. Stefanits H, et al. GABAA receptor subunits in the human amygdala and hippocampus: Immunohistochemical distribution of 7 subunits. J Comp Neurol. 2018;526:324–48.
46. Marowsky A, Fritschy JM, Vogt KE. Functional mapping of GABA A receptor subtypes in the amygdala. Eur J Neurosci. 2004;20:1281–9.
47. Heldt SA, Ressler KJ. Training-induced changes in the expression of GABAA-associated genes in the amygdala after the acquisition and extinction of Pavlovian fear. Eur J Neurosci. 2007;26:3631–44.
48. Dias R, et al. Evidence for a significant role of alpha 3-containing GABAA receptors in mediating the anxiolytic effects of benzodiazepines. J Neurosci. 2005;25:10682–8.
49. Möhler H. The GABA system in anxiety and depression and its therapeutic potential. Neuropharmacology. 2012;62:42–53.
50. Atack JR. GABAA receptor alpha2/alpha3 subtype-selective modulators as potential nonsedating anxiolytics. Curr Top Behav Neurosci. 2010;2:331–60.
51. Engin E, Liu J, Rudolph U. α2-containing GABA(A) receptors: a target for the development of novel treatment strategies for CNS disorders. Pharmacol therapeutics. 2012;136:142–52.
52. Collins I, et al. 3-Heteroaryl-2-pyridones: Benzodiazepine site ligands with functional delectivity for alpha 2/alpha 3-subtypes of human GABA(A) receptor-ion channels. J Med Chem. 2002;45:1887–900.
53. Miller BH, et al. Quantitative trait locus analysis identifies Gabra3 as a regulator of behavioral despair in mice. Mammalian genome: official journal of the International Mammalian Genome. Society. 2010;21:247–57.
54. Koh MT, Rosenzweig-Lipson S, Gallagher M. Selective GABA(A) alpha5 positive allosteric modulators improve cognitive function in aged rats with memory impairment. Neuropharmacology. 2013;64:145–52.
55. Prevot T, et al. Novel Benzodiazepine-like ligands with various anxiolytic, antidepressant, or pro-cognitive profiles. Molecular. Mol Neuropsychiatry. 2019;5:84–97.
56. Sigurdsson T, Duvarci S. Hippocampal-prefrontal interactions in cognition. Behav Psychiatr Dis Front Syst Neurosci. 2016;9:190–190.

57. Koh MT, Rosenzweig-Lipson S, Gallagher M. Selective GABA(A) α5 positive allosteric modulators improve cognitive function in aged rats with memory impairment. Neuropharmacology. 2013;64:145–52.
58. Prevot, TD, et al. Reversal of Age-Related Neuronal Atrophy by α5-GABAA Receptor Positive Allosteric Modulation. Cereb Cortex, 2020;31:1395–1408.
59. Rudolph U, et al. Benzodiazepine actions mediated by specific gamma-aminobutyric acid(A) receptor subtypes. Nature. 1999;401:796–800.
60. Li G, et al. Synthesis of chiral GABA(A) receptor subtype selective ligands as potential agents to treat schizophrenia as well as depression. Arkivoc. 2018;2018:158–82.
61. Billakota S, et al. Personalized medicine: Vinpocetine to reverse effects of GABRB3 mutation. Epilepsia. 2019;60:2459–65.
62. Kirsch GE, et al. Electrophysiology-based assays to detect subtype-selective modulation of human nicotinic acetylcholine receptors. ASSAY Drug Dev Technol. 2016;14:333–44.
63. Bayliss MK, Frick LW. High-throughput pharmacokinetics: Cassette dosing. Curr Opin Drug Disco Devel. 1999;2:20–5.
64. Stamenic TT, et al. Ester to amide substitution improves selectivity, efficacy and kinetic behavior of a benzodiazepine positive modulator of GABAA receptors containing the alpha5 subunit. Eur J Pharm. 2016;791:433–43.
65. Obradovic A, et al. Sh-I-048A, an in vitro non-selective super-agonist at the benzodiazepine site of GABAA receptors: The approximated activation of receptor subtypes may explain behavioral effects. Brain Res. 2014;1554:36–48.
66. Di L, et al. Optimization of a higher throughput microsomal stability screening assay for profiling drug discovery candidates. J Biomolecular Screen. 2003;8:453–62.
67. Prevot TD, et al. Residual avoidance: A new, consistent and repeatable readout of chronic stress-induced conflict anxiety reversible by antidepressant treatment. Neuropharmacology. 2019;153:98–110.
68. Nollet, M, Guisquet AM Le, Belzung C. Models of depression: unpredictable chronic mild stress in mice. Curr Protoc Pharmacol. 2013;5:Unit 5.65.
69. Faucher P, et al. Hippocampal injections of Oligomeric Amyloid β-peptide (1-42) induce selective working memory deficits and long-lasting alterations of ERK signaling pathway. Front Aging Neurosci. 2015;7:245.
70. Wu CC, et al. Selective vulnerability of dentate granule cells prior to amyloid deposition in PDAPP mice: digital morphometric analyses. Proc Natl Acad Sci USA. 2004;101:7141–6.
71. Guilloux J-P, et al. Integrated behavioral z-scoring increases the sensitivity and reliability of behavioral phenotyping in mice: Relevance to emotionality and sex. J Neurosci Methods. 2011;197:21–31.
72. Sekhon BS. Exploiting the power of stereochemistry in drugs: An overview of racemic and enantiopure drugs. J Mod Med Chem. 2013;1:10–36.
73. Nguyen LA, He H, Pham-Huy C. Chiral drugs: An overview. Int J Biomed Sci: IJBS. 2006;2:85–100.
74. Srinivas NR, Barbhaiya RH, Midha KK. Enantiomeric drug development: Issues, considerations, and regulatory requirements. J Pharm Sci. 2001;90: 1205–15.
75. Budău M, et al. Chirality of modern antidepressants: An overview. Adv Pharm Bull. 2017;7:495–500.
76. Zarate, CA, Commentary on the Canadian Network for Mood and Anxiety Treatments (CANMAT) Task Force Recommendations for the Use of Racemic Ketamine in Adults with Major Depressive Disorder. Canadian J Psychiatry. 2021:66:573–539.
77. Henry ME, et al. A comparison of brain and serum pharmacokinetics of R-fluoxetine and racemic fluoxetine: A 19-F MRS study. Neuropsychopharmacology. 2005;30:1576–83.
78. Gorman JM, Korotzer A, Su G. Efficacy comparison of escitalopram and citalopram in the treatment of major depressive disorder: pooled analysis of placebo-controlled trials. CNS Spectr. 2002;7:40–4.
79. Perez-Caballero L, et al. Fluoxetine: a case history of its discovery and preclinical development. Expert Opin Drug Disco. 2014;9:567–78.
80. Bezchlibnyk-Butler K, Aleksic I, Kennedy SH. Citalopram-a review of pharmacological and clinical effects. J Psychiatry Neurosci. 2000;25:241–54.
81. Bahji A, Vazquez GH, Zarate CA Jr. Comparative efficacy of racemic ketamine and esketamine for depression: A systematic review and meta-analysis. J Affect Disord. 2021;278:542–55.
82. Möhler H. Pathophysiological aspects of diversity in neuronal inhibition: A new benzodiazepine pharmacology. Dialogues Clin Neurosci. 2002;4:261–9.
83. Abbas AI, et al. Somatostatin interneurons facilitate hippocampal-prefrontal synchrony and prefrontal spatial encoding. Neuron. 2018;100:926–939.
84. Duman CH, Duman RS. Spine synapse remodeling in the pathophysiology and treatment of depression. Neurosci Lett. 2015;601:20–29.
85. Prévôt TD, et al. sst(2)-receptor gene deletion exacerbates chronic stress-induced deficits: Consequences for emotional and cognitive ageing. Prog Neuropsychopharmacol Biol Psychiatry. 2018;86:390–400.
86. Gumuslu E, et al. The antidepressant agomelatine improves memory deterioration and upregulates CREB and BDNF gene expression levels in unpredictable chronic mild stress (UCMS)-exposed mice. Drug Target Insights. 2014;8:11–21.
87. Fee C, et al. Chronic stress-induced behaviors correlate with exacerbated acute stress-induced cingulate cortex and ventral hippocampus activation. Neuroscience. 2020;440:113–29.
88. Hörtnagl H, et al. Patterns of mRNA and protein expression for 12 GABAA receptor subunits in the mouse brain. Neuroscience. 2013;236:345–72.
89. Schulz JM, et al. Dendrite-targeting interneurons control synaptic NMDA-receptor activation via nonlinear α5-GABA(A) receptors. Nat Commun. 2018;9:3576.
90. Serwanski DR, et al. Synaptic and nonsynaptic localization of GABAA receptors containing the alpha5 subunit in the rat brain. J Comp Neurol. 2006;499:458–70.
91. Duveau V, et al. Spatiotemporal specificity of GABAA receptor-mediated regulation of adult hippocampal neurogenesis. Eur J Neurosci. 2011;34:362–73.
92. Deprez F, et al. Partial inactivation of GABAA receptors containing the α5 subunit affects the development of adult-born dentate gyrus granule cells. Eur J Neurosci. 2016;44:2258–71.
93. Brady ML, Jacob TC. Synaptic localization of α5 GABA (A) receptors via gephyrin interaction regulates dendritic outgrowth and spine maturation. Dev Neurobiol. 2015;75:1241–51.
94. Moda-Sava RN, et al. Sustained rescue of prefrontal circuit dysfunction by antidepressant-induced spine formation. Science. 2019;364;eaat8078.
95. Nikolova YS, et al. Shifting priorities: highly conserved behavioral and brain network adaptations to chronic stress across species. Transl Psychiatry. 2018;8:26.
96. Zhang X, et al. Stress-Induced Functional Alterations in Amygdala: Implications for Neuropsychiatric Diseases. Front Neurosci. 2018;12:367–367.
97. Luscher B, Shen Q, Sahir N. The GABAergic deficit hypothesis of major depressive disorder. Mol Psychiatry. 2011;16:383–406.
98. Karolewicz B, et al. Reduced level of glutamic acid decarboxylase-67 kDa in the prefrontal cortex in major depression. Int J Neuropsychopharmacol. 2010;13:411–20.
99. Romeo B, et al. Meta-analysis of central and peripheral γ-aminobutyric acid levels in patients with unipolar and bipolar depression. J Psychiatry Neurosci. 2018;43:58–66.
100. Hasler G, et al. Reduced prefrontal glutamate/glutamine and gamma-aminobutyric acid levels in major depression determined using proton magnetic resonance spectroscopy. Arch Gen Psychiatry. 2007;64:193–200.
101. Antoniuk S, et al. Chronic unpredictable mild stress for modeling depression in rodents: Meta-analysis of model reliability. Neurosci Biobehav Rev. 2019;99:101–16.
102. Mineur YS, Belzung C, Crusio WE. Effects of unpredictable chronic mild stress on anxiety and depression-like behavior in mice. Behav Brain Res. 2006; 175:43–50.
103. Aarts E, et al. The light spot test: Measuring anxiety in mice in an automated home-cage environment. Behav Brain Res. 2015;294:123–30.

ACKNOWLEDGEMENTS

Authors thank Mehrab Ali and Netta Ussyshkin for support with administrative tasks throughout the study. They thank CAMH animal facility staff for the caring for our animals over the study duration. Authors further thank the members from Charles River Laboratories and NeuroDigitech for their contribution to data generation. We also thank Milwaukee Institute for Drug Discovery and University of Wisconsin-Milwaukee's Shimadzu Laboratory for Advanced and Applied Analytical Chemistry for help with spectroscopy and National Science Foundation, Division of Chemistry [CHE-1625735].

AUTHOR CONTRIBUTIONS

TP and ES designed the study. MYM, SR, DS and JMC synthesized the compounds tested in this study. TP and PL performed the behavioral piece. AK and MMS performed the pharmacokinetic piece. Electrophysiology was outsourced to Charles River Laboratories. TP, AB and MM analyzed the data. TP and AB wrote the manuscript.

FUNDING

CAMH Internal Fund (Discovery Fund), awarded to TP at the time of study execution, and the Campbell Family Mental Health Research Institute of CAMH. Chemistry synthesis funded by NIH (DA-043204, R01NS076517) to JMC. The Science Fund of the Republic of Serbia funded the pharmacokinetic study through Grant No. 7749108 NanoCellEmoCog. JMC, MMS, ES and TP are listed inventors on patents covering syntheses and use of the compounds. ES is Founder of Damona Pharmaceuticals, a biopharma dedicated to bring novel GABAergic compounds to the clinic. AB, PL, MM, MYM, SR, DS, and AK report no conflict of interest.

COMPETING INTERESTS

The authors declare no competing interests.

ADDITIONAL INFORMATION

Supplementary information The online version contains supplementary material available at https://doi.org/10.1038/s41386-022-01360-y.

Correspondence and requests for materials should be addressed to Etienne Sibille or Thomas D. Prevot.

Reprints and permission information is available at http://www.nature.com/reprints

Publisher's note Springer Nature remains neutral with regard to jurisdictional claims in published maps and institutional affiliations.